Electronic Supplementary Information

Methane Dry Reforming in a Coking- and Sintering-Free Liquid Alloy-Salt Catalytic System

Qinghai Yang,[‡a] Congquan Zhou, [‡a] Jihong Ni,[a] and Xiaofei Guan[*a]

[a] School of Physical Science and Technology, ShanghaiTech University,

Shanghai, 201210, China.

[‡]These authors contribute equally.

[*]E-mail: guanxf@shanghaitech.edu.cn

Table of Contents:

Table S1 A list of potential reactions taking place in the liquid NiBi-K_2CO_3 catalytic system during the dry reforming of CH_4 with CO_2.

No.	Type of reactions	Chemical equations
1	CH_4 dry reforming	$CH_{4(g)} + CO_{2(g)} \rightarrow 2H_{2(g)} + 2CO_{(g)}$
2	CH_4 pyrolysis	$CH_{4(g)} \rightarrow C_{(s)} + 2H_{2(g)}$
3	Reverse Boudouard	$C_{(s)} + CO_{2(g)} \rightarrow 2CO_{(g)}$
4	Reverse water gas shift	$H_{2(g)} + CO_{2(g)} \rightarrow H_2O_{(g)} + CO_{(g)}$
5	Steam gasification of carbon	$C_{(s)} + H_2O_{(g)} \rightarrow H_{2(g)} + CO_{(g)}$
6	CH_4 steam reforming	$CH_{4(g)} + H_2O_{(g)} \rightarrow 3H_{2(g)} + CO_{(g)}$
7	C oxidation via $K_2CO_{3(l)}$	$1/2K_2CO_{3(l)} + C_{(s)} \rightarrow K_{(g)} + 3/2CO_{(g)}$
8	CO_2 reduction via $K_{(g)}$	$K_{(g)} + CO_{2(g)} \rightarrow 1/2K_2CO_{3(l)} + 1/2CO_{(g)}$
9	CH_4 partial oxidation via $K_2CO_{3(l)}$	$1/2CH_{4(g)} + 1/4K_2CO_{3(l)} \rightarrow H_{2(g)} + 3/4CO_{(g)} + 1/2K_{(g)}$
10	CH_4 oxidation via $K_2CO_{3(l)}$	$1/8CH_{4(g)} + 1/2K_2CO_{3(l)} \rightarrow 1/8H_2O_{(g)} + 5/8CO_{2(g)} + K_{(g)}$
11	$K_2CO_{3(l)}$ decomposition	$K_2CO_{3(l)} \rightarrow K_2O_{(l)} + CO_{2(g)}$
12	H_2 oxidation via $K_2CO_{3(l)}$	$1/2K_2CO_{3(l)} + 1/2H_{2(g)} \rightarrow K_{(g)} + H_2O_{(g)} + 1/2CO_{(g)}$
13	Steam partial reduction via $K_{(g)}$	$K_{(g)} + H_2O_{(g)} \rightarrow KOH_{(l)} + 1/2H_{2(g)}$
14	CO oxidation via $KOH_{(l)}$	$2KOH_{(l)} + CO_{(g)} \rightarrow K_2CO_{3(l)} + H_{2(g)}$
15	Absorption of CO_2 via $KOH_{(l)}$	$2KOH_{(l)} + CO_{2(g)} \rightarrow K_2CO_{3(l)} + H_2O_{(g)}$
16	CH_4 oxidation via H_2O and $KOH_{(l)}$	$CH_{4(g)} + H_2O_{(g)} + 2KOH_{(l)} \rightarrow K_2CO_{3(l)} + 4H_{2(g)}$

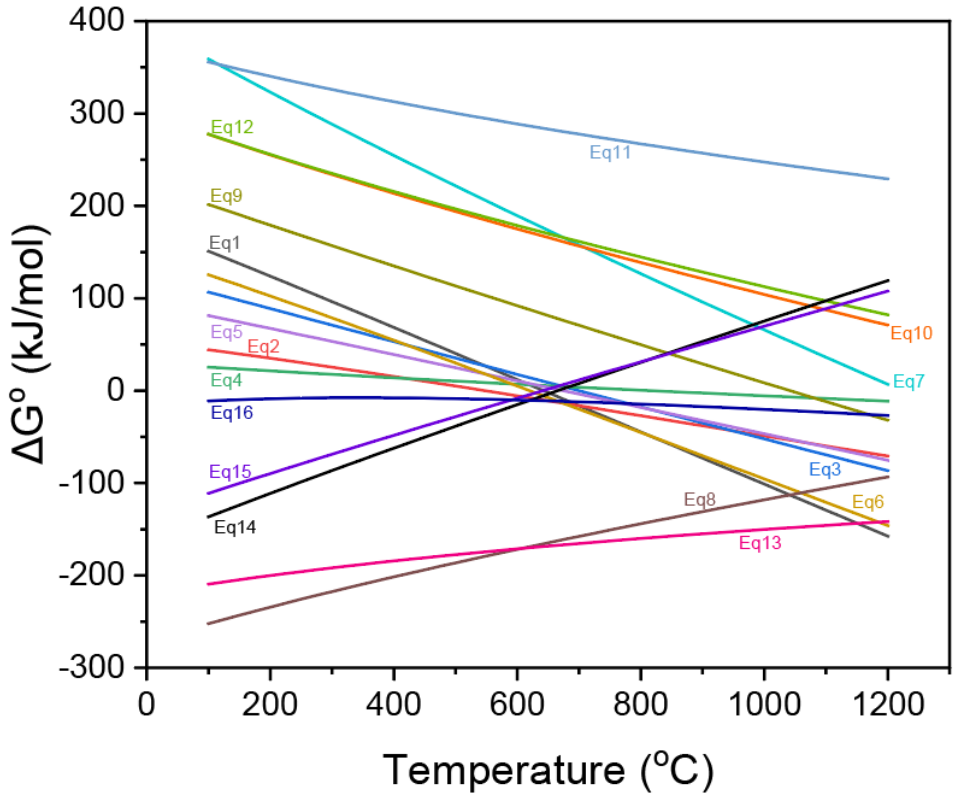

Fig. S1 Standard Gibbs free energy change, ΔG°, (kJ/mol) for the reactions in Table S1. The values of ΔG° are obtained from HSC Chemistry Database.[1]

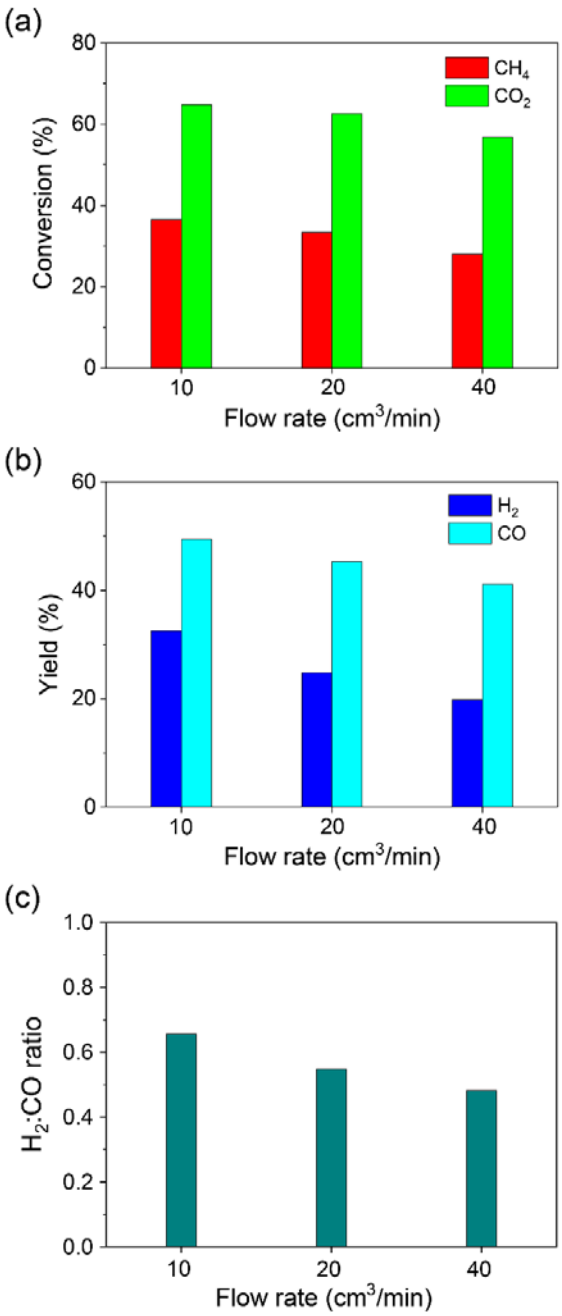

Fig. S2 Effect of the inlet gas flow rate on the catalytic performances of dry reforming with the $Ni_{0.27}Bi_{0.73}$(15cm)-K_2CO_3(15cm) catalytic system at 1000 °C. (a) The conversions of CH_4 and CO_2, (b) the yields of H_2 and CO and (c) the H_2:CO ratio as functions of the flow rate of the equimolar mixture of CH_4 and CO_2.

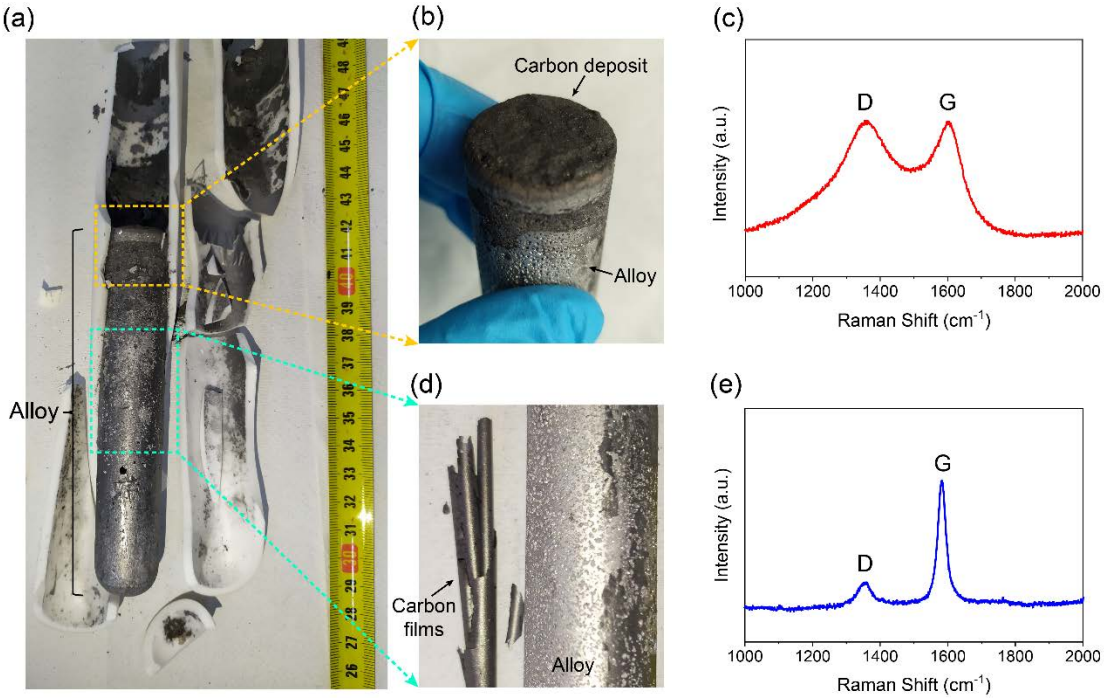

Fig. S3 Carbon production in the dry reforming experiment with 15 cm of $Ni_{0.27}Bi_{0.73}$ alloy as catalyst at 1000 °C for 24 hours with an equimolar mixture of CH_4 and CO_2 at 10 cm^3/min. (a) Photograph of the cooled alloy after opening the alumina reactor. (b) Photograph of the top surface of the cooled alloy. (c) Representative Raman spectrum of the deposit collected from the top of the alloy shows the characteristic peaks at ~1360 and ~1580 cm^{-1} for D and G bands of graphite, respectively. The relative intensity ratio of D and G bands is approximately 1. (d) Photograph of the middle part of the alloy column. Carbon films formed on the interface between the alloy and the alumina reactor via precipitation from the saturated alloy, and some of them readily peeled off. (e) Representative Raman spectrum of the films shows the characteristic peaks for graphite. The relative intensity ratio of D and G bands of the carbon film is much smaller than that of the carbon deposit on the top of alloy, indicating a higher degree of graphitization.[2-3]

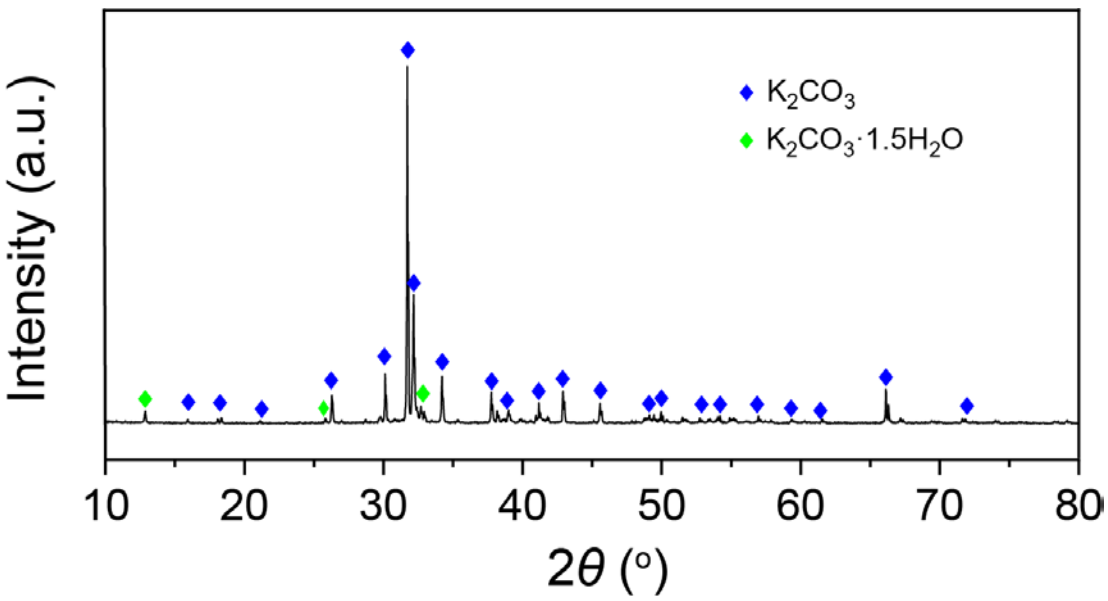

Fig. S4 Representative XRD pattern of the salt samples from the 120-h stability test showing that K_2CO_3 (PDF #01-087-0730) was the main phase with traces of $K_2CO_3 \cdot 1.5H_2O$ (PDF #00-011-0655).

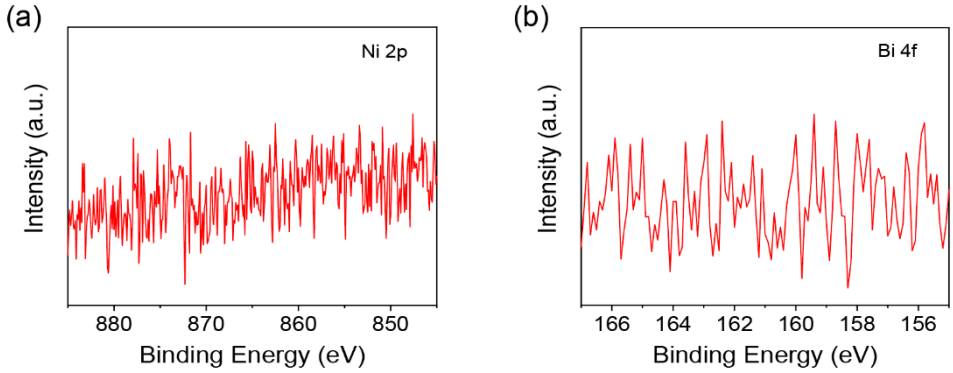

Fig. S5 Representative Ni 2p and Bi 4f XPS spectra of the solidified salt samples.

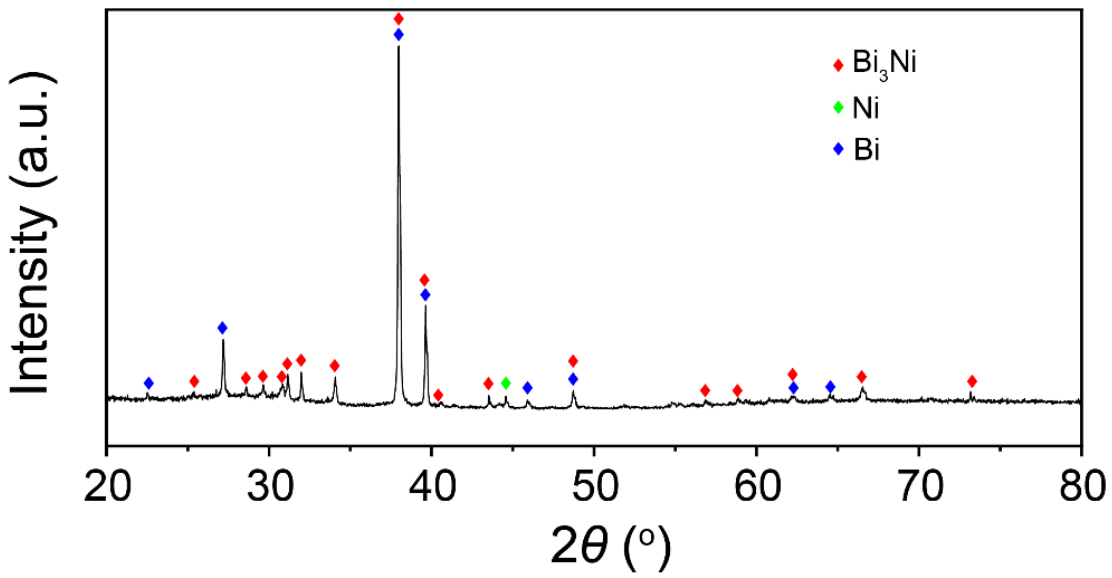

Fig. S6 Representative XRD pattern of the alloy samples after the 120-h stability test showing the characteristic peaks for the crystalline phases of Bi (PDF #00-005-0519), Bi_3Ni (PDF #00-054-0537) and Ni (PDF #04-010-6148).

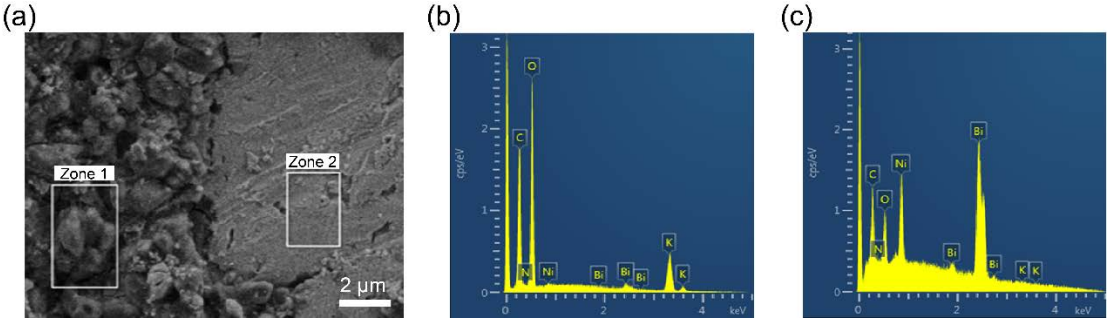

Fig. S7 SEM and EDS results showing that K_2CO_3 was identified in the alloy sample after the dry reforming experiment. (a) SEM image of a solidified alloy sample collected near the middle of the alloy column. (b) EDS analysis for zone 1 showing the presence of K_2CO_3. (c) EDS analysis for zone 2 showing the alloy phase.

References for the Electronic Supplementary Information:

1. Roine, A., HSC Chemistry Database 5.11, Outokumpu Research, Helsinki, Finland, 2002.
2. Ferrari, A.; Robertson, J.; Reich, S.; Thomsen, C., Raman spectroscopy of graphite. Philos. T. Roy. Soc. A. 2004, 362 (1824), 2271-2288.
3. Tallant, D. R.; Friedmann, T. A.; Missert, N. A.; Siegal, M. P.; Sullivan, J. P., Raman Spectroscopy of Amorphous Carbon. Mat. Res. Soc. Symp. Proc. 1997, 498, 37.